Crystallization and characterization of high silica silicoaluminophosphate SAPO-5

S. Seelan, A.K. Sinha*

National Institute of Advanced Industrial Science and Technology, AIST, 1-8-31, Midorigaoka, Ikeda 563-8577, Japan

Abstract

SAPO-5 with a high Si content have been synthesized by using dipropylamine (DPA) as a template in ethylene glycol (EG) (molar ratio of silica in the reaction gels up to 2.4). Crystallinity and silicon incorporation was confirmed by XRD, XRF, N_2 sorption measurement, TG-DTA, SEM, pyridine-TPD and ^{27}Al, ^{29}Si MAS-NMR. These SAPO-5 materials with high Si concentrations show higher activity for toluene alkylation reaction than samples prepared from the gel with up to 0.6 molar ratio of silica.
© 2004 Elsevier B.V. All rights reserved.

Keywords: AlPO-5; SAPO-5; Silicoaluminophosphate; Alkylation

1. Introduction

Silicoaluminophosphate molecular sieves [1] have considerable potential for industrial acidic catalysts [2–4]. They have been found to be effective in *n*-alkane isomerization, *p*-xylene production, olefin oligomerization and isomerization, conversion of methanol to light olefins and alkylation of aromatics [2–4]. For acid catalyzed reactions, it is advantageous to synthesise SAPOs with a high silicon content to increase the number of acidic sites which are located both on dispersed silicon species [5] and at the edge of silicon islands [6]. However, due to poor crystallinity, and formation of large siliceous islands at high Si concentration in the gel, the silicon content in the SAPOs is limited [7,8]. It is advantageous therefore to look for synthesis procedures that allow the synthesis of highly siliceous SAPOs from a gel containing high concentration of silica [7]. Insufficient and non-specific incorporation of Si in the $AlPO_4$ lattice and poor crystallinity of the SAPOs [9–11] are major problems faced during the synthesis of SAPOs.

Numerous efforts have been made in the past to overcome these problems [12–14] through modifications in synthesis methods, such as the use of biphasic medium [15] and novel structure directing templates [16]. Gradual transport of Si from the solution phase to the growing crystalline phase and better depolymerization of Si species in the gel solution could be important for incorporating more Si in the SAPO structure [8,17]. We have shown that it is possible to synthesize highly crystalline SAPO-5 materials with silica molar ratio of up to 0.8 in the initial gel using dipropylamine (DPA) as a template and gradual heating the initial gel [7]. Non-aqueous media have been found to slow down the transport of silicon during crystallization as well as favoring depolymerization of Si due to high pH of the gel which in turn affects the dispersion of silicon in the solid SAPOs [8]. Similar improvement in Mn incorporation in the MnAPO-11 structure is observed during the synthesis in ethylene glycol (EG) [18].

Here we report the synthesis of siliceous SAPO-5 by broadening the SiO_2 concentration in the synthesis gel (Si_{gel}), using the DPA as the organic template, and EG as the synthesis medium. Slow heating of the synthesis gel to the crystallization temperature was used to obtain high crystallinity.

2. Experimental

Aluminium isopropoxide (98%, Aldrich), orthophosphoric acid (85%, Merck), fumed silica (Cabosil) and dipropylamine (DPA; 99%, Aldrich) were used in the syntheses of the SAPOs.

* Corresponding author. Present address: Materials Department, Toyota Central R&D Labs Inc., 41-1 Yokomichi, Nagakute-Cho, Aichi-Gun, Aichi 480-1192, Japan. Tel.: +81-561-63-7683; fax: +81-561-63-6137.
E-mail address: e1258@mosk.tytlabs.co.jp (A.K. Sinha).

Crystalline SAPO-5 materials were prepared by using non-aqueous solvent, EG, from gels with molar composition Al_2O_3: P_2O_5: (0.4–2.4) SiO_2: 5 DPA: 60 EG (gel pH 6.8–7.3). In a typical procedure for the non-aqueous synthesis, 11.6 g of aluminium isopropoxide (98%, Aldrich) was added slowly to 109.7 g of EG under stirring and the mixture was stirred further for 1 h. DPA, 14.2 g (99%, Aldrich), was added dropwise to the stirred mixture which was further stirred for 0.5 h. Then, 11.5 g of orthophosphoric acid was added dropwise and stirring was continued for another 0.5 h. Finally, 0.34 g of fumed silica (Cabosil) was added and the final mixture was stirred for 2 h to obtain a homogeneous gel. The gel was charged into an autoclave (150 ml) and heated at 1.5 K/min to 433 K and then at 0.5 K/min to 473 K without agitation. The final temperature (473 K) was maintained for 48 h to complete the crystallization. The autoclave was then quenched and the products were filtered, washed with distilled water, dried at 383 K and finally calcined at 793 K in air for 8 h.

X-ray powder diffraction (XRD) patterns were recorded on a Rigaku D/MAX-rb diffractometer employing Ni-filtered Cu Kα radiation (λ = 1.5404 Å). The relative crystallinities (%) of the samples synthesized by different methods was obtained by summing the areas of six major diffraction peaks in the 2θ region from 5 to 45°. Solid-state MAS-NMR spectra were recorded on a Bruker MSL-300 spectrometer. ^{29}Si MAS-NMR spectra were measured at a spinning rate of 2.3 kHz, spectral width of 20 kHz, pulse length of 2 ms, delay of 2 s and spectrometer frequency of 59.6 MHz, tetramethylsilane (TMS) was used as the external standard. ^{27}Al MAS-NMR spectra were measured at a spectral width of 125 kHz, pulse length of 1 ms, delay of 500 ms and spectrometer frequency of 78.2 MHz using $Al(H_2O)_6^{3+}$ in a nitric acid solution of $Al(NO_3)_3$ as the external standard. The size and morphology of the samples were examined by scanning electron microscopy (Leica Stereoscan 440). The surface areas were determined by the BET method using a Micromeritics ASAP 2010 instrument. Chemical compositions were determined by XRF analysis. The acidities of the samples were determined by temperature-programmed desorption of pyridine using the reported procedure [19].

Alkylation of toluene was carried out in a fixed-bed, down-flow, tubular glass reactor under atmospheric pressure using 2.0 g of catalyst (10–20 mesh). The catalyst was activated at 823 K in air and flushed in N_2 before each run. The reactants were fed at a weight hourly space velocity (WHSV) of 3 h^{-1}. The products of the reaction were analyzed by a gas chromatograph (Shimadzu; Bentone column, FID detector).

3. Results and discussions

All SAPO-5 samples showed X-ray diffraction patterns corresponding to that of the AFI topology reported previously [20]. The most crystalline sample with 0.6 mol ratio
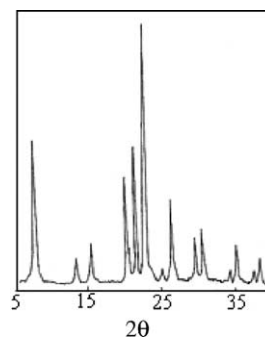

Fig. 1. XRD pattern of calcined, high Si content SAPO-5, synthesized from gel with Si_{gel} = 2.0.

of Si loading in the starting gel (Si_{gel}) was taken as the reference for the calculation of the percentage of crystallinity. The X-ray diffractogram of a high silica content sample (Si_{gel} = 2.0) is shown in Fig. 1. The absence of any extraneous diffraction lines from those reported previously [11] and a base line free of background indicate the high purity and crystallinity of the prepared samples. Table 1 shows the unit cell composition and XRD crystallinity (%) of calcined SAPO-5 samples. The unit cell composition was calculated from XRF analysis, and confirms the silicon content in the calcined samples is in the range 0.11–0.53, from the gels with Si molar ratios (Si_{gel}) varying in the range 0.4–2.4. Gels with Si_{gel}, 2.6 and higher, resulted in less crystalline samples. All SAPO-5 preparations with Si_{gel} up to 2.4 showed a high degree of crystallinity and high pore volumes (based on N_2-sorption capacity) of 0.10–0.15 ml/g with surface areas of 140–180 m^2 g^{-1} after calcination, indicating good thermal stability. It seems that the incorporation of Si in the AFI framework increases its thermal stability.

TG–DTA analysis demonstrated that the sample with a lower Si content (Si_{gel} = 0.6) showed a weight loss of 5.7 wt.% in the temperature range 733–853 K while the sample with higher Si content (Si_{gel} = 2.0) showed a weight loss

Table 1
Si concentration in gel, composition and crystallinity of SAPO-5 samples

Si_{gel} (mole ratio)	Unit cell composition[a]	XRD crystallinity[b] (%)	Surface area (m^2 g^{-1})
0.4	$(Al_{0.50}P_{0.39}Si_{0.11})O_2$	83.5	141
0.6	$(Al_{0.47}P_{0.31}Si_{0.22})O_2$	100	177
0.8	$(Al_{0.43}P_{0.32}Si_{0.25})O_2$	98.7	169
1.0	$(Al_{0.42}P_{0.29}Si_{0.29})O_2$	91.3	ND
1.2	$(Al_{0.38}P_{0.30}Si_{0.32})O_2$	98.2	165
1.4	$(Al_{0.40}P_{0.27}Si_{0.33})O_2$	97.1	159
1.6	$(Al_{0.35}P_{0.28}Si_{0.37})O_2$	98.3	ND
1.8	$(Al_{0.34}P_{0.25}Si_{0.41})O_2$	94.7	ND
2.0	$(Al_{0.30}P_{0.24}Si_{0.46})O_2$	97.8	163
2.2	$(Al_{0.27}P_{0.24}Si_{0.49})O_2$	96.0	153
2.4	$(Al_{0.24}P_{0.25}Si_{0.51})O_2$	93.3	ND

[a] By XRF analysis for calcined sample.
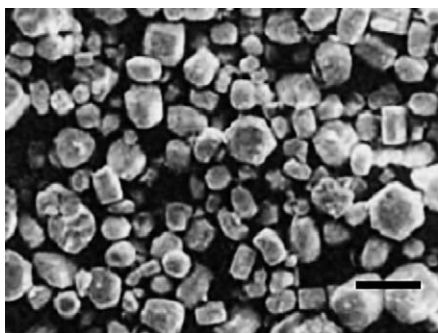[b] Based on most intense XRD peak taking sample Si_{gel} = 0.6 as the reference.

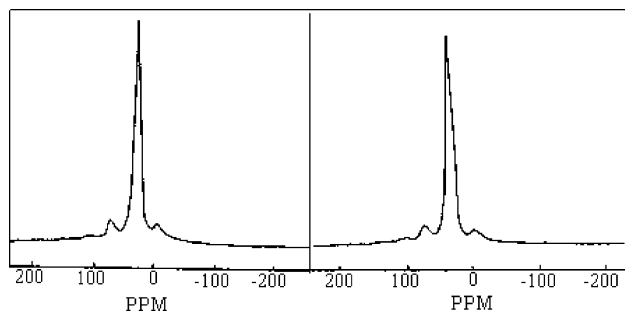Fig. 2. SEM image of the calcined SAPO-5, synthesized from gel with $Si_{gel} = 2.0$ (scale bar = 10 μm).

Fig. 3. ^{27}Al MAS-NMR spectra of calcined SAPO-5: (a) from gel with $Si_{gel} = 0.6$; (b) from gel with $Si_{gel} = 2.0$.

of 6.9% in the temperature range 763–893 K. The average total loss in the higher temperature range which is attributed to the decomposition/combustion of DPA was higher for the higher Si content sample ($Si_{gel} = 2.0$) than the loss from samples with a lower Si content ($Si_{gel} = 0.6$). SEM micrographs (Fig. 2) show the size and morphology of the calcined sample with $Si_{gel} = 2.0$. All particles were uniform with hexagonal and/or elongated shape, having an average diameter of around 5–10 μm.

^{27}Al MAS NMR spectral analysis of the SAPO-5 samples from synthesis gel with $Si_{gel} = 0.6$ (Fig. 3a) and $Si_{gel} = 2.0$ (Fig. 3b) show identical spectra with a unique signal at around 39 ppm, assigned to framework tetrahedral aluminum. ^{29}Si MAS-NMR spectral analysis (Fig. 4) was used to analyze the local ordering of silicon in SAPO-5 samples
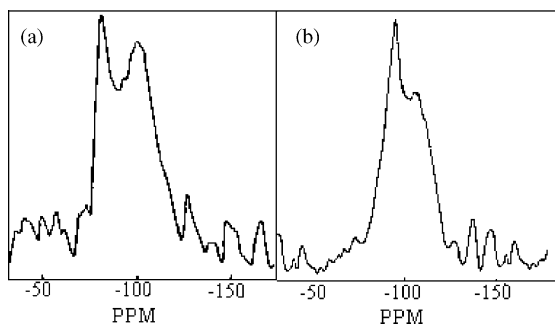
from synthesis gel with $Si_{gel} = 0.6$ (Fig. 2a) and $Si_{gel} = 2.0$ (Fig. 4b). Two peaks at $\delta -91.6$ (Fig. 4a) or $\delta -92.5$ (Fig. 4b) and at $\delta -109.3$ (Fig. 4a) or $\delta -105.0$ (Fig. 4b) indicates the presence of multiple Si environments in the samples. Resonance peak around $\delta -90$ is generally assigned to Si(4Al) type isolated silicon species, peaks around 110 are assigned to Si(0Al) type silicon species present in silica islands, while peaks around $\delta -95, -98, -104$ are assigned to Si(1Al), Si(2Al) and Si(3Al) type of silicon species [21,22], respectively. ^{29}Si MAS-NMR spectra for the samples with high and low Si contents indicates that both samples contain Si atoms present as isolated species as well as in silica islands. Broad nature of spectrum is also indicative of the presence of Si species at the edge of Si islands and coordinated with different number of Al atoms (1Al, 2Al, 3Al) in these samples.

The total acidities of the samples measured by temperature programmed desorption of pyridine showed that acidity in terms of amount of pyridine desorbed (per gram of catalyst) beyond 573 K was 117 μmol g^{-1} (23% of ideal value based on elemental analysis) and 148.0 μmol g^{-1} (11% of ideal value based on elemental analysis), respectively, for the samples with $Si_{gel} = 0.6$ and $Si_{gel} = 2.0$, indicating higher acidities in samples with higher Si contents.

Alkylation of toluene with methanol produces, primarily, a mixture of xylenes, the distribution of which in the product largely depends on the characteristics of the catalyst. Side reactions may also take place, beside alkylation, namely, disproportionation and/or transalkylation. Besides, trimethylbenzenes (TMBs) are also formed. Results of the acid catalyzed toluene alkylation reaction using methanol over the catalysts with a low Si content ($Si_{gel} = 0.6$) and a high Si content ($Si_{gel} = 2.0$) at different reaction temperatures (623, 648 K) are shown in Table 2. It is observed that the toluene conversion is much higher over SAPO-5 samples with a higher Si content which can be attributed to its higher acidity as determined by pyridine-TPD. The samples with a higher Si content show the formation of higher amounts of total xylenes along with the TMBs. The toluene conversion is higher at higher reaction temperatures for both the samples. There is no observed difference in shape-selectivity between these catalysts as the p-xylene/o-xylene ratios are 0.6 and 0.7, respectively, for high and low Si content

Fig. 4. ^{29}Si MAS-NMR spectra of calcined SAPO-5: (a) from gel with $Si_{gel} = 0.6$; (b) from gel with $Si_{gel} = 2.0$.

Table 2
Toluene alkylation over SAPO-5 samples (time on stream = 3 h; WHSV = 3 h^{-1}, toluene:methanol = 1:1(mole))

	SAPO-5(Si = 0.6)		SAPO-5(Si = 2.0)	
	623 K	648 K	623 K	648 K
Conversion (%)	22.31	25.95	36.43	42.38
Product distribution (wt.%)				
Benzene	0.83	0.95	1.26	1.71
Total xylenes	16.26	18.46	27.69	32.06
TMB[a]	5.22	6.54	7.48	8.61

[a] Total trimethylbenzenes.

catalysts. The para to ortho ratio in xylene will be affected by the presence of strong acid sites which are the active site for the isomerization of xylene but we do not observe much difference, indicating that the acid strengths of the two types of catalysts may not be quite different.

4. Conclusions

Highly crystalline SAPO-5 samples with very high Si contents (up to 2.4 molar ratio in gel) could be synthesized by using non-aqueous ethylene glycol as the synthesis medium and by heating the synthesis gel gradually to the crystallization temperature. These samples contain multiple silicon environments and have higher acidity and higher activity for acid catlyzed toluene alkylation reaction than the SAPO-5 samples with lower Si contents. Such high silica containing SAPOs are potentially useful as catalyst for acid catalyzed reactions.

References

[1] B.M. Lok, C.A. Messina, R.L. Patton, R.T. Gajek, T.R. Cannan, E.M. Flanigen, US Patent 4,40,871 (1984); J. Am. Chem. Soc. 106 (1984) 6092.
[2] R.J. Pellet, P.K. Coughlin, G.N. Long, J.A. Rabo, US Patent 4880,760 (1989).
[3] F.P. Gortsema, A.R. Springer, G.N. Long, US Patent 4,880,700 UOP (1989).
[4] F.P. Gortsema, K.J. Pellet, A.R. Springer, J.A. Rabo, G.N. Long, US Patent 4,913,799 (1990).
[5] G. Sastre, D.W. Lewis, C.R.A. Catlow, J. Phys. Chem. B 101 (1997) 5249.
[6] D. Barthomeuf, Zeolites 14 (1994) 394.
[7] A.K. Sinha, S. Sainkar, S. Sivasanker, Micropor. Mesopor. Mater. 31 (1999) 321.
[8] A.K. Sinha, S. Sivasanker, P. Ratnasamy, Ind. Eng. Chem. Res. 37 (1998) 2208.
[9] C.S. Blackwell, R.L. Patton, J. Phys. Chem. 92 (1988) 3965.
[10] U. Lohse, F. Vogt, J. Richter-Mendau, Cryst. Res. Technol. 28 (1993) 1101.
[11] P.A. Barrett, R.H. Jones, J.M. Thomas, G. Sankar, I.J. Shannon, C.R.A. Catlow, J. Chem. Soc. Chem. Commun. (1996) 2001.
[12] P.S. Singh, R. Bandyopadhyay, B.S. Rao, J. Chem. Soc., Far. Trans. 92 (1996) 2017.
[13] R. Vomscheid, M. Briend, M.J. Peltre, P.P. Man, D. Barthomeuf, J. Phys. Chem. 98 (1995) 9614.
[14] B. Herreros, J. Klinowski, J. Phys. Chem. 99 (1995) 9514.
[15] M. Montoya-Urbina, D. Cardoso, J. Perez-Pariente, E. Sastre, T. Blasco, V. Fornes, J. Catal. 173 (1998) 501.
[16] Q. Gao, S. Li, R. Xu, J. Chem. Soc. Chem. Comm. (1994) 1465.
[17] N. Venkatathri, S.G. Hegde, P.R. Rajmohanan, S. Sivasanker, J. Chem. Soc. Faraday Trans. 93 (1997) 3411.
[18] A.K. Sinha, D. Srinivas, S. Sivasanker, Catal. Lett. 61 (1999) 193.
[19] V.R. Choudhary, V.S. Nayak, Appl. Catal. A: Gen. 4 (1983) 31.
[20] http://www.zeolites.ethz.ch/zeolites/xrdpatterns/afi.
[21] S. Ashtekar, S.V.V. Chilukuri, D.K. Chakraborty, J. Phys. Chem. 98 (1994) 4878.
[22] L.S. de Saldarriaga, C. Saldarriaga, M.E. Davis, J. Am. Chem. Soc. 109 (1987) 2686.